

Original articles

Research article

<https://doi.org/10.17308/kcmf.2023.25/11482>**GaN micro- and nanostructures selectively grown on profiled sapphire substrates using PA-MBE without lithography**A. N. Semenov¹✉, D. M. Nechaev¹, S. I. Troshkov¹, D. S. Berezina¹, A. S. Abbas², V. N. Jmerik¹¹Ioffe Institute,
26 Politekhnikeskaya st., St. Petersburg 194021, Russian Federation²King Abdulaziz City for Science and Technology (KACST),
King Abdullah Rd, Al Raed, Riyadh 12354, Saudi Arabia**Abstract**

Purpose: Development of technology for the formation of ordered arrays of nanocolumns (NCs) of GaN microcrystals using plasma-activated molecular beam epitaxy from nitrogen (PA-MBE) on profiled sapphire substrates (SPS) of large diameter with a micro-cone profile. The proposed method eliminates the use of low-performance and expensive nanolithography methods. The article is aimed at a deeper understanding of the processes that determine the growth kinetics of III-N nanocolumns using PA MBE on patterned sapphire substrates with multiple orientations of various non-polar and polar planes.

A new technological process for the fabrication of GaN NCs using PA-MPE is proposed, which ensures selectivity of their growth at the tops of PPS micro-cones and suppresses growth on the semipolar planes of these substrates. GaN NCs and microcrystals were grown using PA-MBE on commercially available PPS.

A technology has been developed for the formation of discharged arrays of GaN nanocolumns without the use of lithographic procedures. Modes have been established that allow the formation of microcrystals and NCs with different diameters: from 30 nm to several microns. A diagram of the growth of GaN by the PA MBE method on PPS has been constructed, demonstrating the boundaries of the technological regimes for the formation of GaN NCs and microcrystals with different surface topography.

Keywords: Selective area growth, Whiskers, Microcrystals, Nanocolumns, Plasma-activated molecular beam epitaxy, Wide-gap semiconductor compounds A³N

Funding: The research was carried out with financial support from the Ministry of Science and Higher Education Higher Education of Russian Federation (agreement 075-15-2022-1224 “Bio-Light”).

For citation: Semenov A. N., Nechaev D. M., Troshkov S. I., Berezina D. S., Abbas A. S., Jmerik V. N. Micro- and nanostructures of GaN selectively grown on patterned sapphire substrates by PA-MBE without lithography techniques. *Condensed Matter and Interphases*. 2023;25(4): 532–541. <https://doi.org/10.17308/kcmf.2023.25/11482>

Для цитирования: Семенов А. Н., Нечаев Д. М., Трошков С. И., Березина Д. С., Аббас А. С., Жмерик В. Н. Микро- и наноструктуры GaN, селективно выращенные на паттернированных сапфировых подложках методом ПА-МПЭ без использования литографии. *Конденсированные среды и межфазные границы*. 2023;25(4): 532–541. <https://doi.org/10.17308/kcmf.2023.25/11482>

✉ Alexey Semenov, e-mail: semenov@beam.ioffe.ru

© Semenov A. N., Nechaev D. M., Troshkov S. I., Berezina D. S., Abbas A. S., Jmerik V. N., 2023



The content is available under Creative Commons Attribution 4.0 License.

1. Introduction

Recently, three-dimensional (3D) nano- and microcrystals based on group III metal nitrides A^3N (BN, AlN, GaN, InN) with a predominant orientation along the c or $-c$ axes, which are also commonly called nanocolumns (NCs) or nanowires, have been widely studied. Such structures are important both for fundamental studies of the properties of III-N compounds and for the creation of new electronic and optoelectronic devices based on them. In the latter case, nanocolumnar heterostructures can significantly improve the parameters of light-emitting and photo-receiving devices operating in various spectral ranges [1–4]. Highly efficient LEDs in the visible and ultraviolet (UV) ranges, respectively, have been successfully implemented based on InGaN/GaN and GaN/AlGaIn “core-shell” heterostructures [5–10]. In particular, based on NC AlN structures, Zhao et al. [9] demonstrated the shortest wavelength UV LEDs emitting at a wavelength $\lambda = 207$ nm, which showed not only high structural perfection due to the absence of threading dislocations in them, but also high efficiency of TM-polarized radiation output through the upper c -plane individual NCs [11]. In addition, an increased efficiency of p-doping with Mg atoms was discovered for AlGaIn NCs compared to planar layers of the same composition [12]. And finally, NCs in the A^3N material system are promising for the development of new types of emitters, including sources of single photons in the visible and UV ranges [13–16].

One of the main requirements for the design of most device structures based on NCs is their regular arrangement on the surface of the substrate with varying distances between individual NCs - from a minimum ~ 1 μm (in LEDs) to several microns (in single photon sources). To solve this problem, methods for spatially selective epitaxial growth of A^3N -based NCs have been developed, in which the formation of preferred nucleation sites for group III adatoms is achieved using nano-lithographic operations on the surface of various dielectric masks. Most of these works use the processes of nanoimprinting [17] or electron beam lithography [18, 19]. The selectivity of NC growth is ensured due to its occurrence in open areas of nano-masks, i.e. on the surface of underlying substrates, with its complete

absence on the surface of mask dielectrics. These methods provide spatial resolution from several hundred to tens of nanometers and are also characterized by relatively high spatial selectivity and uniformity of NC growth. However, these methods also have some disadvantages. For electron beam lithography, this is, first of all, the low productivity of the method, which precludes its use in the industrial production of devices on large-diameter substrates. The high cost of nanoimprinting matrices also hinders the widespread use of this method. Despite the success of nano-lithographic methods, the technological problems of ensuring high homogeneity of structures on large-area substrates and achieving sufficient growth selectivity with suppression of parasitic growth in the spaces between NCs have not yet been fully resolved [14]. In addition, all nano-lithographic methods are characterized by edge effects associated with excessive accumulation of adatoms near the edge of the dielectric mask. Finally, the resistive masks made of organic materials used in these methods can serve as a source of contamination of the NCs.

To solve the above problems, an active search is underway for methods for growing regularly distributed NCs without the use of nano-lithographic processes [20–25]. In our previous works [20–22], for the selective growth of A^3N NCs by plasma-activated molecular beam epitaxy (PA MBE), it was proposed to use patterned c -sapphire substrates (PPS) with individual micro-cones with characteristic values of base diameters, heights and distances between the peaks are several microns. Such substrates are relatively easy to fabricate using standard photolithographic methods and wet etching of commercial planar c -sapphire substrates [26]. Currently, PPS are used mainly for the manufacture of LED heterostructures, the efficiency of which increases due to the effects of reducing the concentrations of extended defects (dislocations) and improving the output of radiation through the semipolar planes of such substrates [27].

In our work [21], we demonstrated the possibility of selective growth of nitrogen-polar GaN(000-1) NCs using the PA MBE method in nitrogen-enriched conditions at the tops of PPS micro-cones and presented a qualitative model that describes such growth taking into

account the features of thermodynamics (surface energy) and surface mobility of adatoms on various polar and semipolar crystallographic planes. The influence of the PPS geometry, the roughness of the initial surface, the substrate temperature, and the ratio of the fluxes of group 3 atoms (Ga) to activated nitrogen Ga/N_2^* on the growth kinetics of single NCs was studied. These studies identified the important role of the initial growth stages in promoting selective growth of GaN NCs. In addition, the influence of the In flow as a surfactant on the growth of light-emitting NCs with InGaN/GaN quantum wells (QWs) was studied and the optimal ratios of the fluxes of all growth flows and substrate temperature were determined, ensuring maximum selectivity for the growth of GaN NCs, as well as the formation of InGaN/GaN QWs in them [22]. The use of PPS for selective growth of A³N microcolumns has been demonstrated by other groups. In particular, recent work by Ahn et al. [25], this approach was used to obtain GaN NCs with a diameter of several microns on such substrates using metal-organic vapor phase epitaxy. In this work, varying the diameters of the microcone apices was achieved using pre-epitaxial chemical-mechanical polishing of PPS, during which the flat apices expanded.

This paper presents the results of a study of the characteristics of GaN growth by PA MBE on PPS with microcones in a wide range of varying growth temperatures and the ratio of gallium and plasma-activated nitrogen fluxes. Changing the growth parameters made it possible to vary

the size of GaN NCs in a wide range from several tens of nm to 1 μm , and also to move from the growth of conventional cylindrical (hexagonal) NCs to the growth of microcrystals with a complex topology of polar and semi-polar crystallographic planes.

2. Experimental section

The samples were grown by PA-MBE on commercially available PPS with microcones with a base diameter of 2 μm , a height of 1.4 μm , and a distance between them of 2.1 μm , as shown in the images obtained using a scanning electron microscope (SEM) and shown in Fig. 1.

Before the start of growth of GaN NCs, the substrates were annealed at a temperature of 800 $^\circ\text{C}$ and nitrided at the same temperature in an active nitrogen flow of 0.5 Monolayers (ML)/sec (where thickness 1 ML = 0.25 nm), calibration of which was carried out by measuring the growth rate of AlN into metal-enriched conditions. Then, in all samples, GaN nucleation layers were grown under gallium-enriched conditions with a flux ratio of $Ga/N_2^* = 2.2$ ($N_2^* = 0.1\text{ML/s}$) at a substrate temperature of 760 – 770 $^\circ\text{C}$. The thickness of this layer in the planar regions of the PPS was ~ 55 nm. Further growth of GaN NCs was carried out using two modes, differing primarily in the values of gallium (Ga) fluxes at the same active nitrogen flux ($N_2^* = 0.4\text{ML/s}$). In the first mode, the growth of two samples was carried out under nitrogen-enriched conditions with the same Ga/N_2^* flux ratio ~ 0.25 and at different substrate temperatures (see below) for 4 hours in pulsed

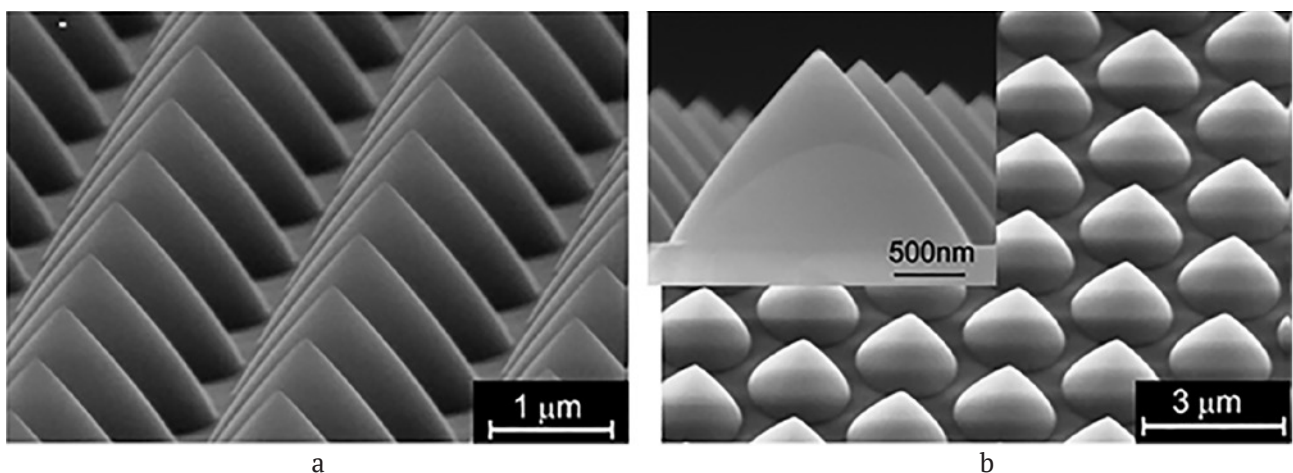


Fig. 1. SEM images of the initial micro-cone-shaped patterned c-sapphire substrate (μ -CPSS) surface (a) cross section of the μ -CPSS with micro-cones and (b) general view of the μ -CPSS surface

mode with growth interruption every 30 seconds by the blocking of all growth fluxes using the main shutter. During this growth interruption for 30 s, an increase in the substrate temperature was observed almost linearly from the initial (growth) values of 760 °C and 780 up to 785 °C and 805 °C, respectively. Temperature values were measured using an infrared pyrometer. After NC growth, some of the samples were etched in a KOH solution (10%) for 10 minutes at 20 °C. In the second mode, GaN NCs were grown on the same PPS for 5 hours under Ga-enriched growth conditions at $Ga/N_2^* \sim 1.5$ (without taking into account Ga desorption) and various substrate temperatures from 695 to 795 °C. In all NC growth processes described above, an indium flux of $In = 0.2\text{--}0.4$ ML/sec was used as a surfactant.

The surface topographies of GaN NCs were studied using a CamScan 4-88-DV-100 SEM.

3. Results and discussion

3.1. Selective growth of GaN NCs on PPS under nitrogen-enriched conditions

In this work, compared with our previous work [21], to increase the selectivity of GaN NC

growth (i.e., suppress the growth of parasitic NCs on the side faces of micro-cones) and reduce their diameter, relatively low Ga fluxes ($Ga \sim 0.1$ ML/s) and low flux ratios ($Ga/N_2^* = 0.25$). In addition, in our opinion, the increase in selectivity was facilitated by the transition from a constant to a pulsed growth mode with short-term annealing of the sample to stimulate the upward diffusion of Ga atoms to the top of the microcones. An increase in the substrate temperature by 20 °C allowed a larger number of adatoms to reach the tops of the PPS microcones. The high degree of spatial selectivity in the growth of GaN NCs with a height of 500 – 700 nm and a diameter of up to 35 nm was confirmed by their SEM images in Fig. 2a-c. Note that in previous work [21], the typical diameters of GaN NCs were 50–100 nm. However, NC growth was observed only at relatively low substrate temperatures of 760/785 °C during NC growth/annealing, respectively, and when temperature was increased to 780/805 °C, there was no growth of NCs on the tops of the PPS, as evidenced by the SEM images in Fig. 2d,e. We associate the lack of growth with increasing temperature with an increase in the desorption

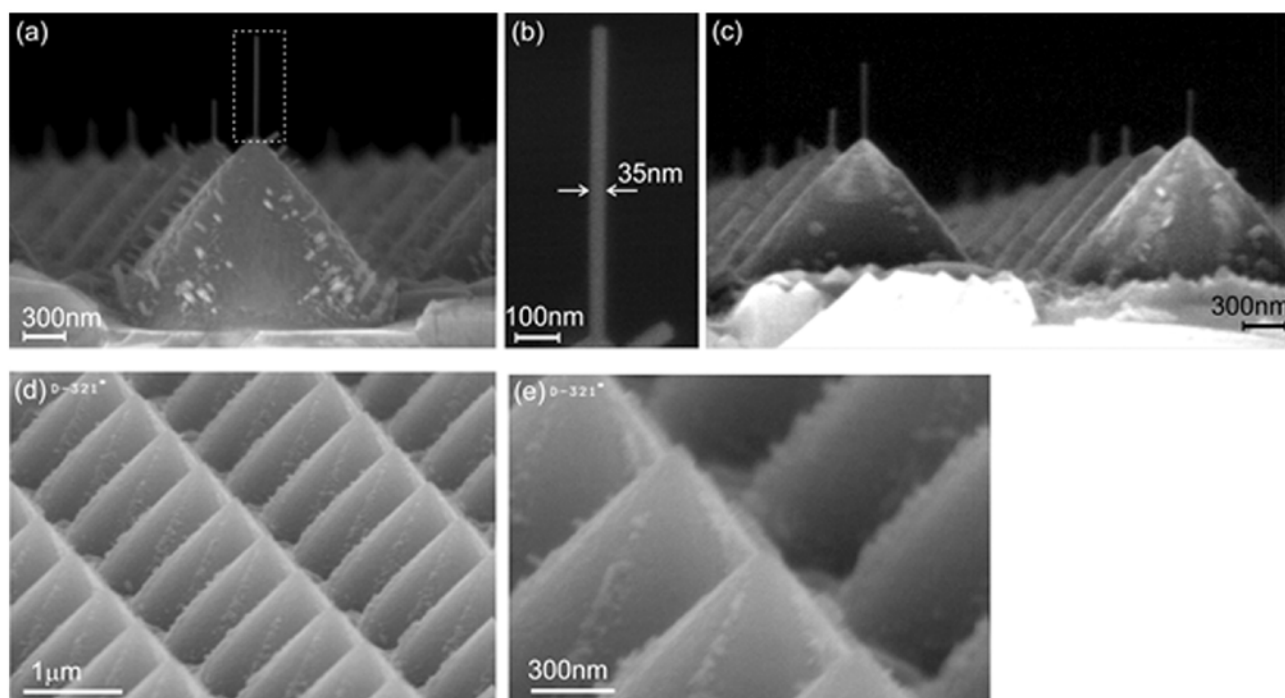


Fig. 2. SEM images of GaN NCs grown using nitrogen-enriched conditions ($Ga/N_2^* = 0.25$) and short-term growth interruptions with increasing temperature from 760 to 785 °C (a-c) and from 780 to 805 °C (d, e). (a) – general view of NC after growth; (b) – enlarged image of the NC, highlighted in (a) with a dotted line; (c) – General view of the NC after etching in KOH

of Ga atoms and the thermal decomposition of GaN NCs.

Unfortunately, the nucleation of GaN NCs at the tops of the PPS was of a probabilistic nature and the growth of NCs was not observed at every vertex even at relatively low substrate temperatures, as shown in Fig. 2a. This is most likely due to the scatter in the parameters of the substrates and the absence of flat nanoregions with a (0001) orientation on some vertices, on which NCs with nitrogen polarity [000-1] nucleate [21]. Note also that the formation of parasitic GaN NCs of smaller height, which were directed perpendicular to these planes, was also observed on the semipolar planes of the PPS.

The samples after etching in KOH did not reveal significant changes in the shape of the NCs at the tops of the PPS, but complete etching (i.e., disappearance) of the parasitic NCs on

the semipolar planes was observed. This result demonstrates the relatively slow etching of polarly oriented GaN [000-1] on NC vertices and confirms the high chemical stability of non-polar {1-100} planes to etching in KOH solutions, as recently demonstrated by Tautz et al. [28].

2.2. Growth of GaN on PPS under metal-enriched conditions

Fig. 3 shows SEM images of microcrystals and NCs formed under the same Ga-enriched conditions ($Ga/N_2^* = 1.5$) at a substrate temperature varying from 695 to 795 °C. In the images of all GaN micro- and nanocrystals, complete correspondence was observed between their density and the density of the original micro-cones on the surface of the PPS. Moreover, at low growth temperatures (695–707 °C), many (>50%) of the top parts of GaN microcrystals had

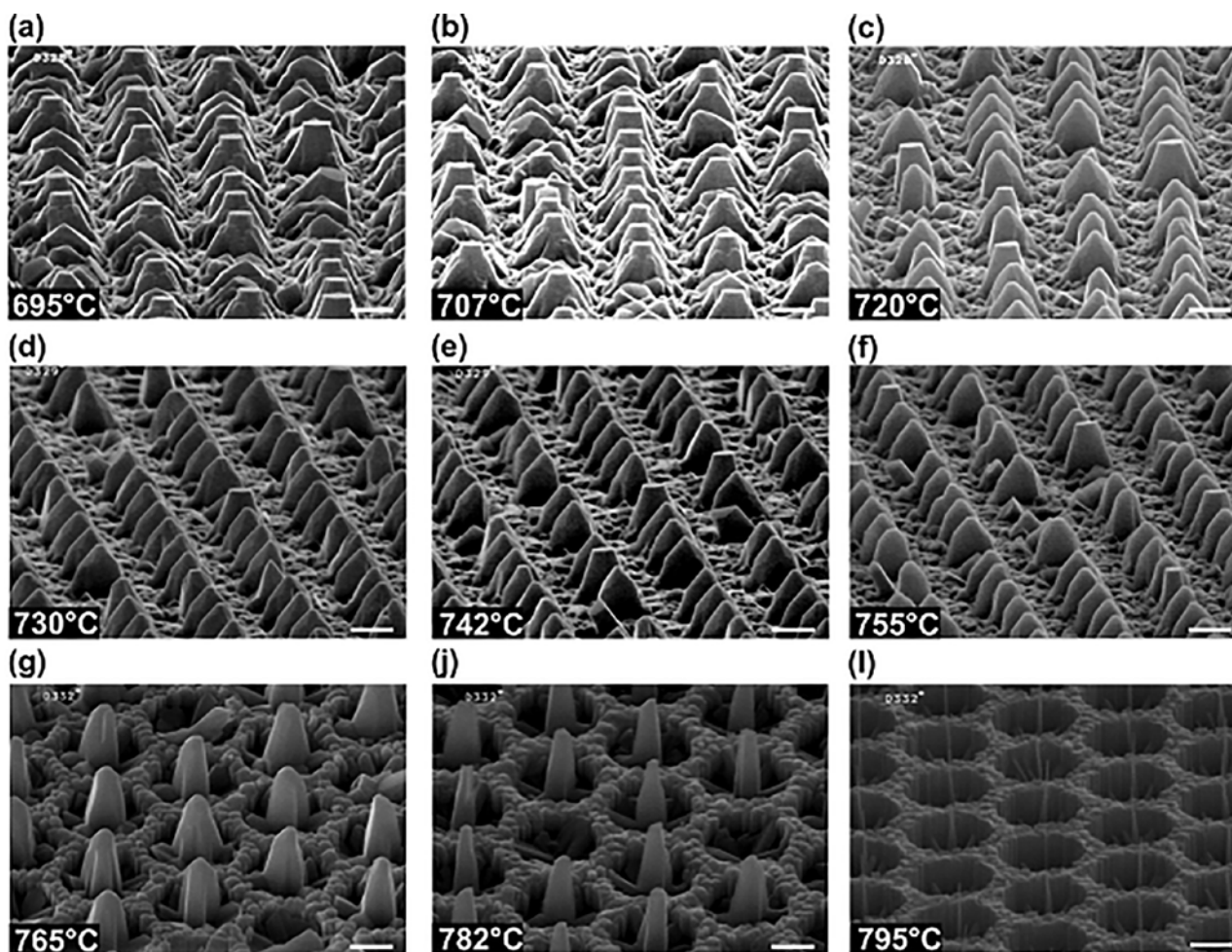


Fig. 3. SEM images of GaN micro- and nanocrystals grown in Me-(Ga) enriched conditions ($Ga/N_2^* = 1.5$) at different substrate temperatures: (a) – 695 °C, (b) – 707 °C, (c) – 720 °C, (d) – 730 °C, (e) – 742 °C, (f) – 755 °C, (g) – 765 °C, (h) – 782 °C, (i) – 795 °C

the shape of hexagonal parallelepipeds with a height of ~ 300 nm and flat tops with a diameter of ~ 0.5 μm , as shown in Fig. 3a, b.

As the growth temperature increased up to 755 $^{\circ}\text{C}$, a decrease in the number of such GaN microcrystals with flat tops was observed, the diameters of which also decreased and, moreover, a pencil-like cut of the tops was observed, as shown in Fig. 3b-f. A further increase in temperature to 795 $^{\circ}\text{C}$ led to a decrease in the diameter of GaN microcrystals until the transition to the growth of single nanocolumns with a diameter decreasing in the direction of the vertices down to a minimum diameter of <50 nm. Importantly, these single NCs were precisely located at the centers of regular micro-holes with a diameter of 2 μm (i.e., in full accordance with the topology of the PPS cones). GaN layers grown on flat areas of the PPS form a “honeycomb” flat surface morphology, as shown in Fig. 3g-i.

Fig. 4a-c show cross-sectional images of cleavages of several structures with GaN NCs grown at different substrate temperatures, the general appearance of which is shown in Fig. 3. Figure 4a shows that the growth of GaN at low temperatures (695 $^{\circ}\text{C}$) begins at the top of the PPS in the form of an inverted pyramid (i.e., with the

top oriented downward) similar to the hexagonal pyramids that we observed in a similar work on the growth of InN on PPS in metal-enriched conditions [20].

During the growth of this pyramid, when it reached a height of ~ 1 μm , its inclined (semi-polar) growth planes mirrored their orientation, and growth continued in the form of a normally oriented pyramid (i.e., with the apex at the top). However, when this pyramid reached a height of about 1 μm , the angle of the inclined planes changed again and further growth of GaN occurred in the form of a hexagonal flat-topped pyramid oriented in the vertical direction. Note that simultaneously with this growth from the tops of the PPS, growth of GaN was also observed on inclined (semi-polar) planes perpendicular to them, as shown in Fig. 4a. On flat areas of the PPS surface, continuous GaN layers with a relatively smooth surface topography grew in comparison with the rough topography of layers grown on the same flat areas of PPS under nitrogen-enriched conditions (see Fig. 2a).

With an increase in the growth temperature, first of all, a decrease in the diameters of the NCs and a transition to their more vertically oriented growth of the side walls was observed.

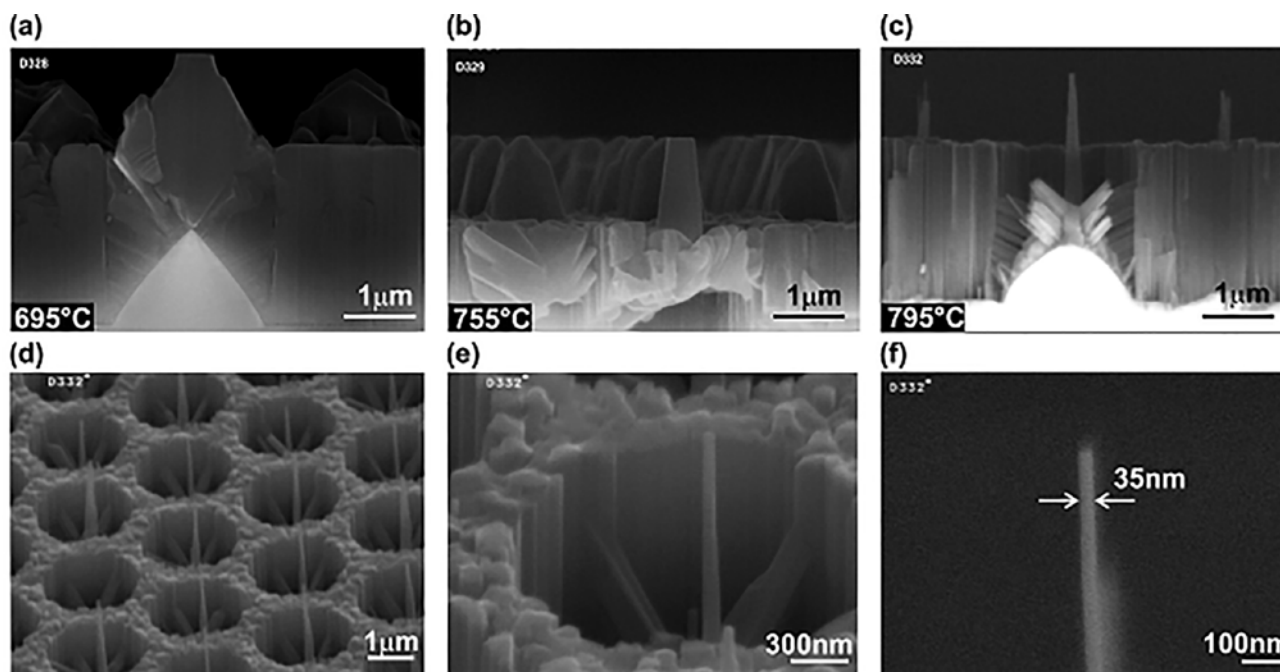


Fig. 4. SEM images of cross sections of GaN microcrystals and NCs grown in Ga-enriched conditions ($Ga/N_2^* = 1.5$) at different substrate temperatures: (a) – 695 $^{\circ}\text{C}$, (b) – 755 $^{\circ}\text{C}$, (c) – 795 $^{\circ}\text{C}$. (d-f) – SEM images with different magnifications of the last NC (c), grown at a maximum substrate temperature of 795 $^{\circ}\text{C}$

At the same time, in the region of average substrate temperatures (720–765 °C), the NCs demonstrated a change in the angle of inclination of the walls. However, in the sample grown at the maximum temperature in this work, 795 °C, the NC diameter varied from ~250 nm at the base to 35 nm at the top, with a NC height of more than 2 μm. It is important that the growth rate of the NCs significantly exceeded the growth rate of the bulk GaN layer above the flat PPS region, which over five hours of growth led to the heights of the NC tops exceeding the level of the continuous layer by approximately 1 μm. Thus, a series of experiments on the growth of GaN on PPS using PA MBE under significantly different growth conditions showed the possibility of significantly varying the shape of growing NCs and micro(nano) crystals.

According to Wulff's theorem, the equilibrium shape of any crystal is determined by the minimum surface energy of its faces—differently oriented crystallographic planes [29]. For the hexagonal semiconductor compound GaN, first-principles calculations show significantly lower surface energies of the non-polar [1-100] and [11-20] planes compared to the polar and semi-polar planes [0001], [000-1], [11-22], [1-101], [1-102], etc. [30]. Therefore, GaN NCs under equilibrium conditions should demonstrate preferential vertical growth in one of two polar directions - [0001] or [000-1]. The results of this work on the growth of N-polar GaN NCs on PPS under highly nitrogen-enriched PA MBE conditions generally confirm the above conclusion (see Fig. 2) and are fully consistent with the results of our previous work [21].

The growth of such NCs under metal-enriched conditions at high substrate temperatures (~800 °C) was discovered for the first time, and its important feature is the growth of NCs on almost all the tops of PPS micro-cones, in contrast to NCs that randomly form on the same vertices under nitrogen-enriched conditions. It should also be noted that it is possible to form GaN micro- and nanocrystals of complex shapes with multiple faces of semi-polar orientation through their growth in Ga-enriched conditions at low and medium substrate temperatures (695–720 °C and 720–765 °C, respectively).

The results on the growth of GaN NCs on PPS under Me-enriched conditions indicate a

significant role of the kinetic factors of PA MPE in this growth regime. Indeed, with an increase in the substrate temperature during the growth of GaN under nominally metal-enriched conditions, one can first assume a significant increase in the rate of thermal desorption of Ga above a temperature of 700 °C (Ga^{TD}), where its value for the [0001] plane exceeds 0.3 ML/s [31,32]. This leads to the disappearance of Ga adsorption layers on the GaN surface (a monolayer for (000-1)-GaN and a bilayer in the case of (0001) GaN growth), providing high mobility of all adatoms and, as a consequence, 2D growth modes with an atomically smooth surface morphology. As the substrate temperature increases (>750 °C), one should expect the onset of thermal congruent decomposition of GaN at a rate of (Ga^{CD}) [33, 34]. These processes lead to a significant change in the effective flux ratio $(Ga - Ga^D - Ga^{CD}) / (N_2^* - N_2^{CD})$, which decreased as the temperature increased. Thus, the shape of a GaN NC is determined not only by the equilibrium values of the surface energies of differently oriented planes. Unfortunately, an accurate quantitative calculation of the growth processes of GaN NCs under nonequilibrium metal-enriched conditions is impossible because in the known literature there are no parameters of thermal desorption and congruent decomposition for various crystalline faces of GaN. Nevertheless, to qualitatively explain the transitions between complex forms of GaN micro- and nanocrystals on PPS, one can use the dependences of the theoretically calculated values of the relative surface energies of various planes on the chemical potential of nitrogen under varying stoichiometric conditions of PA MPE. Such dependencies were constructed in the work of Lee et al. [30] and according to them, only under nitrogen-rich conditions the (000-1)N plane is the most stable, i.e. has lower surface energy compared to the energies of other planes. However, upon transition to Me-enriched conditions (i.e., when the chemical potential of nitrogen decreases), a different relationship between the surface energies of the planes is observed and the semipolar planes {11-2-2}Ga have the lowest energy. This explains the initial growth of inverted pyramids we observed under highly Ga-enriched conditions. These studies of the crystallographic features of GaN growth on

PPS under various PA MBE conditions will be continued in the future. At the present stage of research, it is possible to construct a schematic diagram of various growth modes of GaN NCs on PPS depending on the substrate temperature and the nominal Ga/N_2^* flux ratio, which is presented in Fig. 5.

4. Conclusion

The features of selective area growth of GaN nano- and microcrystals without the use of lithography methods have been studied. The possibilities of such growth using plasma-activated molecular beam epitaxy on profiled c-sapphire substrates with a microcone profile have been demonstrated. It has been shown that when using nitrogen-enriched growth conditions (with a flux ratio of $Ga/N_2^* = 0.25$), an increase in the selectivity of the growth of GaN nanocolumns and a decrease in their diameter to 35 nm (at a height of several hundred nm) is achieved by carrying out the process in a pulsed mode at a temperature substrates 780 °C with short-term annealing, during which the substrate temperature increases by 25 °C. However, in this growth mode, the nucleation of NCs at the tops of microcones is characterized by a probability of no more than 50%.

In the opposite case of metal (Ga)-enriched GaN growth conditions with a flux ratio of $Ga/N_2^* = 1.5$, the growth of nanocrystals is determined by the substrate temperature. At

high values (~800 °C), the formation of GaN nanocolumns with a diameter in the upper part of ~30 nm is observed, which nucleate at almost every vertex of the patterned substrate. Importantly, the tops of individual regular GaN NCs are almost 1 micron higher than the level of the flat GaN layer grown between the microconuses. In the case of lower growth temperatures, the growth of complex micro- and nanocrystals with different surface topologies and orientations of semi-polar side walls is observed. At extremely low growth temperatures (~700 °C), the growth of complex GaN microcrystals is observed, which in the upper part have the regular shape of hexagonal parallelepipeds with flat tops.

Contribution of the authors

A. N. Semenov – concept of the study, text writing, final conclusions, carrying out epitaxial growth; D. V. Nechaev – carrying out epitaxial growths, results discussing and text editing; S. I. Troshkov – SEM measurements of the samples and results discussing; V. N. Zhmerik – ideas, development of methodology, scientific guidance and text editing.

Conflict of interests

The authors declare that they have no known competing financial interests or personal relationships that could have influenced the work reported in this paper.

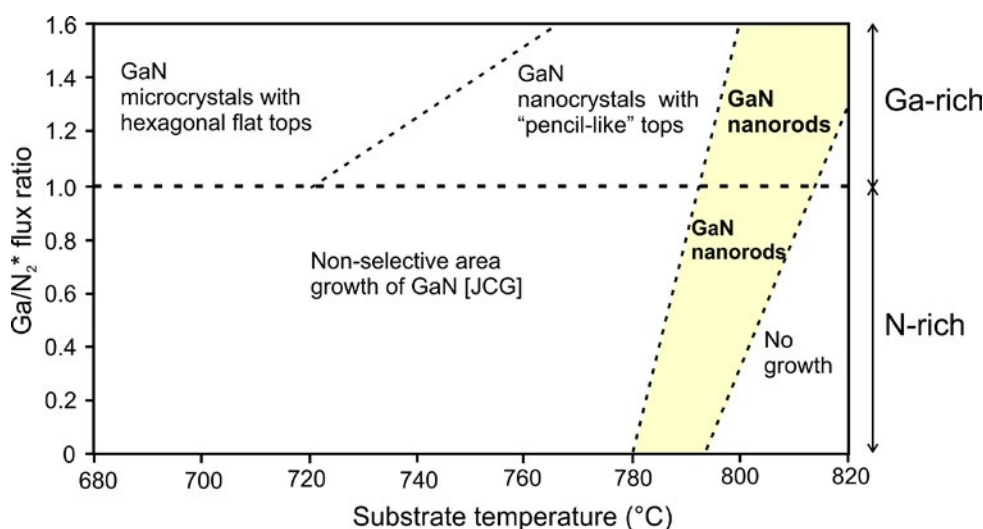


Fig. 5. Schematic diagram of different growth modes of micro-, nanocrystals and GaN nanorods grown by PA-MBE on PSS at different substrate temperatures and Ga/N_2^* flux ratios

References

- Li S., Waag A. GaN based nanorods for solid state lighting. *Journal of Applied Physics*. 2012;111: 071101. <https://doi.org/10.1063/1.3694674>
- Mandl M., Wang X., Schimpke T., ... Strassburg M. Group III nitride core-shell nano- and microrods for optoelectronic applications. *Physica Status Solidi (RRL) – Rapid Research Letters*. 2013;7(10): 800–814. <https://doi.org/10.1002/pssr.201307250>
- Zhao C.; Alfaraaj N.; Subedi R. C., ... Ooi B. S. III-nitride nanowires on unconventional substrates: From materials to optoelectronic device applications. *Progress in Quantum Electronics*. 2018;61: 1–31. <https://doi.org/10.1016/j.pquantelec.2018.07.001>
- Chen F., Ji X., Lau S. P. Recent progress in group III-nitride nanostructures: from materials to applications. *Materials Science and Engineering: R: Reports*. 2020;142: 100578. <https://doi.org/10.1016/j.mser.2020.100578>
- Schimpke T., Mandl M., Stoll I., ... Strassburg M. Phosphor-converted white light from blue-emitting InGa_N microrod LEDs. *Physica Status Solidi A*. 2016;213(6): 1577–1584. <https://doi.org/10.1002/pssa.201532904>
- Sun H., Li X. Recent advances on III-nitride nanowire light emitters on foreign substrates – toward flexible photonics. *Physica Status Solidi A*. 2019;216: 1800420. <https://doi.org/10.1002/pssa.201800420>
- Meier J., Bacher G. Progress and challenges of InGa_N/Ga_N-based core-shell microrod LEDs. *Materials*. 2022;15: 1626. <https://doi.org/10.3390/ma15051626>
- Adhikari S., Kremer F., Lysevych M., Jagadishae C., Tan H. H. Core-shell Ga_N/AlGa_N nanowires grown by selective area epitaxy. *Nanoscale Horizons*. 2023;8: 530. <https://doi.org/10.1039/d2nh00500j>
- Zhao S., Djavid M., Mi Z. Surface emitting, high efficiency near-vacuum ultraviolet light source with aluminum nitride nanowires monolithically grown on silicon. *Nano Letters*. 2015;15: 7006–7009. <https://doi.org/10.1021/acs.nanolett.5b03040>
- Mi Z., Zhao S., Woo S. Y., ... Botton G. A. Molecular beam epitaxial growth and characterization of Al(Ga)_N nanowire deep ultraviolet light emitting diodes and lasers. *Journal of Physics D: Applied Physics*. 2016;49: 364006. <https://doi.org/10.1088/0022-3727/49/36/364006>
- Djavid M., Mi Z. Enhancing the light extraction efficiency of AlGa_N deep ultraviolet light emitting diodes by using nanowire structures. *Applied Physics Letters*. 2016;108: 051102. <https://doi.org/10.1063/1.4941239>
- Zhao C., Ebaid M., Zhang H., ... Ooi B. S. Quantified hole concentration in AlGa_N nanowires for high-performance ultraviolet emitters. *Nanoscale*. 2018;10: 15980–15988. <https://doi.org/10.1039/C8NR02615G>
- Holmes M. J., Choi K., Kako S., Arita M., Arakawa Y. Room-temperature triggered single photon emission from a III-nitride site-controlled nanowire quantum dot. *Nano Letters*. 2014;14(2): 982–986. <https://doi.org/10.1021/nl404400d>
- Yamamoto T., Maekawa M., Imanishi Y., Ishizawa S., Nakaoka T., Kishino K. Photon correlation study of background suppressed single InGa_N nanocolumns. *Japanese Journal of Applied Physics*. 2016;55: 04EK03. <https://doi.org/10.7567/JJAP.55.04EK03>
- Mäntynen H., Anttu N., Sun Z., Lipsanen H. Single-photon sources with quantum dots in III–V nanowires. *Nanophotonics*. 2019;8(5): 747–769. <https://doi.org/10.1515/nanoph-2019-0007>
- Arakawa Y., Holmes M. J. Progress in quantum-dot single photon sources for quantum information technologies: A broad spectrum overview. *Applied Physics Reviews*. 2020;7: 021309. <https://doi.org/10.1063/5.0010193>
- Dai J., Liu B., Zhuang Z., ... Xie, Fabrication of AlGa_N nanorods with different Al compositions for emission enhancement in UV range. *Nanotechnology*. 2017;28: 385205. <https://doi.org/10.1088/1361-6528/aa7ba4>
- Nami M., Eller R. F., Okur S., Rishinaramangalam A. K., Liu S., Brener I., Feezell D. F. Tailoring the morphology and luminescence of Ga_N/InGa_N core-shell nanowires using bottom-up selective-area epitaxy. *Nanotechnology*. 2017;28: 025202. <https://doi.org/10.1088/0957-4484/28/2/025202>
- Hasan S. M. N., You W., Ghosh A., Sadaf S. Md., Arafin S. Selective area epitaxy of Ga_N nanostructures: MBE growth and morphological analysis. *Crystal Growth & Design*. 2023. <https://doi.org/10.1021/acs.cgd.2c01506>
- Shubina T. V., Pozina G., Jmerik V. N., ... Ivanov S. V. III-nitride tunable cup-cavities supporting quasi whispering gallery modes from ultraviolet to infrared. *Scientific Reports*. 2015;5: 17970. <https://doi.org/10.1038/srep17970>
- Jmerik V. N., Kuznetsova N. V., Nechaev D. V., ... Ivanov S. V. Selective area growth of N-polar Ga_N nanorods by plasma-assisted MBE on micro-cone-patterned c-sapphire substrates. *Journal of Crystal Growth*. 2017;477: 207–211. <https://doi.org/10.1016/j.jcrysgro.2017.05.014>
- Semenov A. N., Nechaev D. V., Troshkov S. I., ... Ivanov S. V. Features of the selective growth of Ga_N nanorods on patterned c-sapphire substrates of various configurations. *Semiconductors*. 2018;52(13): 1770–1774. <https://doi.org/10.1134/S1063782618130158>
- Kim J., Choi U., Pyeon J., So B., Nam O. Deep-ultraviolet AlGa_N/Al_N core-shell multiple quantum wells on Al_N nanorods via lithography-free method.

Scientific Reports. 2018;8: 935. <https://doi.org/10.1038/s41598-017-19047-6>

24. Shen J., Yu Y., Wang J., Zheng Y., Gan Y., Li G. Insight into the Ga/In flux ratio and crystallographic plane dependence for MBE self-assembled growth of InGaN nanorods on patterned sapphire substrates. *Nanoscale*. 2020;12(6): 4018–4029. <https://doi.org/10.1039/c9nr09767h>

25. Ahn M. J., Jeong W. S., Shim K. Y., ... Byun D. Selective-area growth mechanism of GaN microrods on a plateau patterned substrate. *Materials*. 2023;16: 2462. <https://doi.org/10.3390/ma16062462>

26. Wang J., Guo L. W., Jia H. Q., ... Zhou J. M. Fabrication of patterned sapphire substrate by wet chemical etching for maskless lateral overgrowth of GaN. *Journal of the Electrochemical Society*. 2006;153(3): C182. <https://doi.org/10.1149/1.2163813>

27. Takano T., Mino T., Sakai J., Noguchi N., Tsubaki K., Hirayama H. Deep-ultraviolet light-emitting diodes with external quantum efficiency higher than 20% at 275 nm achieved by improving light-extraction efficiency. *Applied Physics Express*. 2017;10: 031002. <https://doi.org/10.7567/APEX.10.031002>

28. Tautz M., Weimar A., Graßl C., Welzel M., Díaz D. D. Anisotropy and mechanistic elucidation of wet-chemical gallium nitride etching at the atomic level. *Physica Status Solidi A*. 2020;217(21): 2000221. <https://doi.org/10.1002/pssa.202000221>

29. Sun Q., Yerino C. D., Leung B., Han J., Coltrin M. E. Understanding and controlling heteroepitaxy with the kinetic Wulff plot: A case study with GaN. *Journal of Applied Physics*. 2011;110: 053517. <https://doi.org/10.1063/1.3632073>

30. Li H., Geelhaar L., Riechert H., Draxl C. Computing equilibrium shapes of wurtzite crystals: the example of GaN. *Physical Review Letters*. 2015;115: 085503. <https://doi.org/10.1103/PhysRevLett.115.085503>

31. Jmerik V. N., Nechaev D. V., Ivanov S. V. Kinetics of metal-rich PA molecular beam epitaxy of AlGaIn heterostructures for mid-UV photonics. In: *Molecular beam epitaxy (second edition)*. M. Henini (ed.). Elsevier; 2018. pp. 135–179. <https://doi.org/10.1016/B978-0-12-812136-8.00008-6>

32. Koblmüller G., Averbek R., Riechert H., Pongratz P. Direct observation of different equilibrium Ga

adlayer coverages and their desorption kinetics on GaN (0001) and (000-1) surfaces. *Physical Review B*. 2004;69: 035325. <https://doi.org/10.1103/PhysRevB.69.035325>

33. VanMil B. L., Guo H., Holbert L. J., ... Myers T. H. High temperature limitations for GaN growth by RF-plasma assisted molecular beam epitaxy: Effects of active nitrogen species, surface polarity, and excess Ga-overpressure. *Physica Status Solidi (c)*. 2005;2(7): 2174–2177. <https://doi.org/10.1002/pssc.200461573>

34. Fernández-Garrido S., Koblmüller G., Calleja E., Speck J. S. In situ GaN decomposition analysis by quadrupole mass spectrometry and reflection high-energy electron diffraction. *Journal of Applied Physics*. 2008;104: 033541. <https://doi.org/10.1063/1.2968442>

Information about the authors

Alexey N. Semenov, Cand. Sci. (Phys.–Math.), Senior Researcher, Ioffe Institute (St. Petersburg, Russian Federation).

<https://orcid.org/0000-0002-0719-0236>
semenov@beam.ioffe.ru

Dmitii V. Nechayev, Cand. Sci. (Phys.–Math.), Senior Researcher, Ioffe Institute (St. Petersburg, Russia).

<https://orcid.org/0000-0003-4420-8420>
nechayev@mail.ioffe.ru

Sergei I. Troshkov, Cand. Sci. (Phys.–Math.), Senior Researcher, Ioffe Institute (St. Petersburg, Russia).

<https://orcid.org/0000-0002-3307-6226>
S.Troshkov@mail.ioffe.ru

Darya S. Berezina, postgraduate student, Young Researcher, Ioffe Institute (St. Petersburg, Russia).

<https://orcid.org/0000-0001-9190-1768>
Dariya.Burenina@mail.ioffe.ru

Abbas Arwa Saud, Ph.D, Researcher, King Abdulaziz City for Science and Technology (Riyadh, Saudi Arabia).

arwasaudabdullah@gmail.com

Valentin Nikolaevich Jmerik, Dr. Sci. (Phys.–Math.), Professor, Chief Researcher, Ioffe Institute (St. Petersburg, Russia).

<https://orcid.org/0000-0001-8759-7273>
jmerik@pls.ioffe.ru

Received 10.10.2023; approved after reviewing 13.10.2023; accepted for publication 16.10.2023; published online 25.12.2023.

Translated by the author of the article